nature geoscience

LETTERS

PUBLISHED ONLINE: 4 DECEMBER 2011 | DOI: 10.1038/NGEO1327

Anthropogenic and natural warming inferred from changes in Earth's energy balance

Markus Huber and Reto Knutti*

The Earth's energy balance is key to understanding climate and climate variations that are caused by natural and anthropogenic changes in the atmospheric composition. Despite abundant observational evidence for changes in the energy balance over the past decades[1–3], the formal detection of climate warming and its attribution to human influence has so far relied mostly on the difference between spatio-temporal warming patterns of natural and anthropogenic origin[4–6]. Here we present an alternative attribution method that relies on the principle of conservation of energy, without assumptions about spatial warming patterns. Based on a massive ensemble of simulations with an intermediate-complexity climate model we demonstrate that known changes in the global energy balance and in radiative forcing tightly constrain the magnitude of anthropogenic warming. We find that since the mid-twentieth century, greenhouse gases contributed 0.85 °C of warming (5–95% uncertainty: 0.6–1.1 °C), about half of which was offset by the cooling effects of aerosols, with a total observed change in global temperature of about 0.56 °C. The observed trends are extremely unlikely (<5%) to be caused by internal variability, even if current models were found to strongly underestimate it. Our method is complementary to optimal fingerprinting attribution and produces fully consistent results, thus suggesting an even higher confidence that human-induced causes dominate the observed warming.

The optimal fingerprint detection and attribution framework provides a rigorous, statistical method to quantify the contributions of different external forcings and internal variability to the observed climate changes[7]. In essence, it is based on a regression of the observations onto model simulated patterns and relies on the spatio-temporal response patterns from different forcings being clearly distinct. The assumptions are that climate models simulate the spatial patterns reasonably well and that regional responses from different forcings can be scaled and combined linearly. The global energy budget is not necessarily conserved and observed changes in the energy budget are not considered. Previous studies showed that observed patterns of surface air temperature provide a constraint on the human contribution to the observed warming[4]. Here we demonstrate that the global energy balance provides a further strong, comprehensive and physically motivated constraint.

In equilibrium, the Earth emits as much energy by outgoing longwave radiation at the top of the atmosphere as it receives net shortwave radiation from the sun. Robust evidence for recent deviations from that equilibrium comes from a variety of observations and model simulations[1,8]. The most likely value of the current net radiative forcing F is estimated at 1.6 W m^{-2}, compensated by further outgoing longwave radiation λT and energy uptake of the planet Q:

$$F = Q + \lambda T \quad (1)$$

Owing to its large heat capacity, the ocean accounts for more than 85% of the energy content change Q in the climate system[9]. A robust ocean warming trend is evident despite sparse data and uncertainties and biases in ocean observations[3,10]. The feedback parameter λ is inversely related to climate sensitivity[11].

We use a massive ensemble of the Bern2.5D climate model of intermediate complexity[12,13], driven by bottom-up estimates of historic radiative forcing F, and constrained by a set of observations of the surface warming T since 1850 and heat uptake Q since the 1950s (see Methods). The Special Report on Emissions Scenarios (SRES) A2 (ref. 14) emission scenario is used as one illustration of a non-intervention scenario. The radiative forcing time series[15,16] are shown in Fig. 1 along with the probabilistic model output based on the constrained model parameters[17]. The energy balance model has no natural interannual variability but is able to reproduce the observed global trend of past temperature and ocean heat uptake. Uncertainties in surface warming, ocean heat uptake and in all individual radiative forcing components are considered (see Methods).

Figure 2a shows the contribution of different forcing species to the accumulated forcing since the year 1850. The partitioning of the net cumulative forcing into ocean heat uptake and outgoing longwave radiation is illustrated in Fig. 2b. Between 1850 and 2010, the climate system accumulated a total net forcing energy of 140×10^{22} J with a 5–95% uncertainty range of 95–197 $\times 10^{22}$ J, corresponding to an average net radiative forcing of roughly 0.54 (0.36–0.76) W m^{-2}. The additional energy input is balanced in nearly equal parts by ocean heat uptake and outgoing longwave radiation. About 83% of the accumulated energy from carbon dioxide forcing alone of 164 (151–178) $\times 10^{22}$ J is offset by the combined negative direct and indirect effect of aerosols. However, there are large uncertainties for the radiative forcing of aerosols, in particular for the indirect effect. The negative forcings of stratospheric ozone, black and organic carbon, as well as the positive forcings of stratospheric water vapour and nitrous oxide, play only a minor role in the cumulative forcing budget. The positive and negative non-CO_2 forcings are also of similar magnitude. For an A2 scenario, the historic cumulative forcing would be doubled in the next 33 (28–38) years and tripled in 52 (45–60) years.

The model results for 1950–2004 are shown in Fig. 2c,d and compare very well with recent observational estimates[2], partly as a result of calibrating the model to the observed total ocean and surface warming. Although the estimates for most forcing agents are similar, we infer a larger energy flux from variations in solar irradiance as a result of the particular forcing reconstruction used. If anything our estimate of the solar contribution is likely to be overestimated (see Methods). Ocean heat uptake for 3,000 m depth is also larger, but the model is only constrained using data to 700 m depth. Furthermore, uncertainties in ocean heat

Institute for Atmospheric and Climate Science, ETH Zurich, Universitätstrasse 16, 8092 Zurich, Switzerland. *e-mail: reto.knutti@env.ethz.ch.

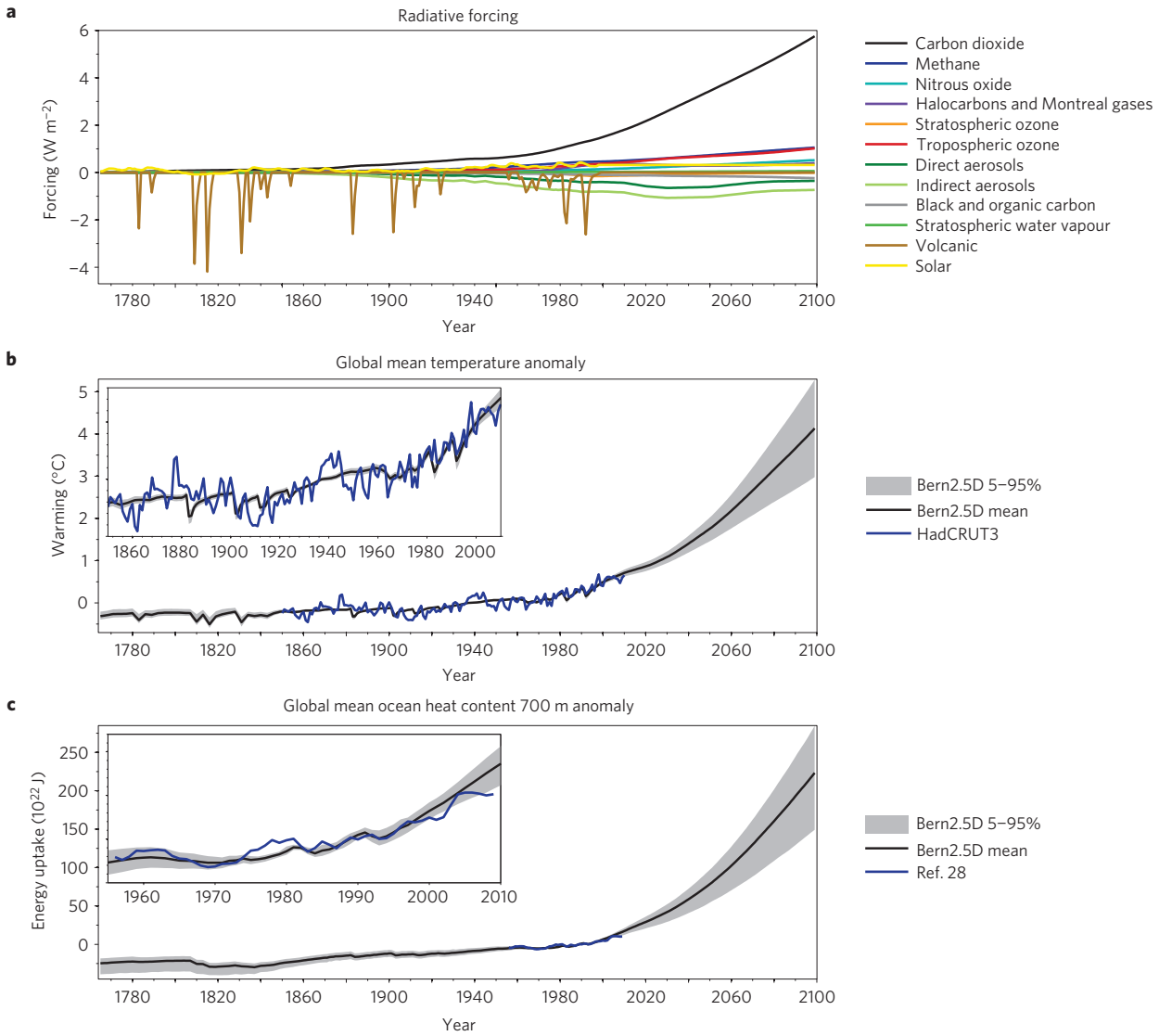

Figure 1 | Radiative forcings and observed and simulated warming using observationally constrained model parameters. a, Radiative forcings from historical reconstructions and the SRES A2 scenario for different forcing agents. **b**,**c**, Emulation of observed global-mean temperature (**b**) and observed ocean heat uptake to 700 m (**c**; ref. 27) with the Bern2.5D climate model. The grey shading denotes the 5–95% uncertainty range.

uptake are large and differences between various reconstructions are significant[18]. The near constant ocean temperature over the past five years are not simulated by the model and its causes remain unclear[10].

The probabilistic contributions of individual forcing agents to past and future decadal changes in global temperature are shown in Fig. 3. We assume that all forcing agents have equal efficacy (see Methods), in contrast to studies using more complex models[19]. The probabilistic ranges presented here account for uncertainties in the observations, radiative forcing, internal variability and model inadequacy (see Methods). The simulated mean temperature increase 2000–2009 compared to 1850–1859 is 0.82 °C, with a 5–95% uncertainty range of 0.72–0.93 °C. The estimate is similar to the observed value of 0.79 °C. Greenhouse gases contributed 1.31 °C (0.85–1.76 °C) to the increase, that is 159% (106–212%) of the total warming. The cooling effect of the direct and indirect aerosol forcing is about −0.85 °C (−1.48 to −0.30 °C). The warming induced by tropospheric ozone and solar variability are of similar size (roughly 0.2 °C). The contributions of stratospheric water vapour and ozone, volcanic eruptions, and organic and black carbon are small.

The individual contributions to the observed temperature increase of about 0.55 °C since the 1950s are illustrated in Fig. 3c. Our total estimate of 0.51 °C (0.45–0.57 °C) is close to the observed temperature change. The largest positive contribution of 0.85 °C (0.57–1.13 °C) is from greenhouse gases and compares well with the values estimated by optimal fingerprint studies[5,6,20] (see Supplementary Information). Expressed as a fraction of the total warming, greenhouse gases contributed 166% (120–215%). The net cooling from the direct and indirect aerosol forcing is −0.45 °C (−0.78 to −0.16 °C), thereby offsetting −44% (−73 to −28%) of the greenhouse induced warming. It is thus extremely likely (>95% probability) that the greenhouse gas induced warming since the mid-twentieth century was larger than the observed rise in global average temperatures, and extremely likely that anthropogenic forcings were by far the dominant cause of warming. The natural forcing contribution since 1950 is near zero.

Similar to earlier studies[13,21], such constrained ensembles can be used for probabilistic temperature projections of future emission scenarios. The contributions to the total warming for the mid-twenty-first century by different radiative forcings are illustrated

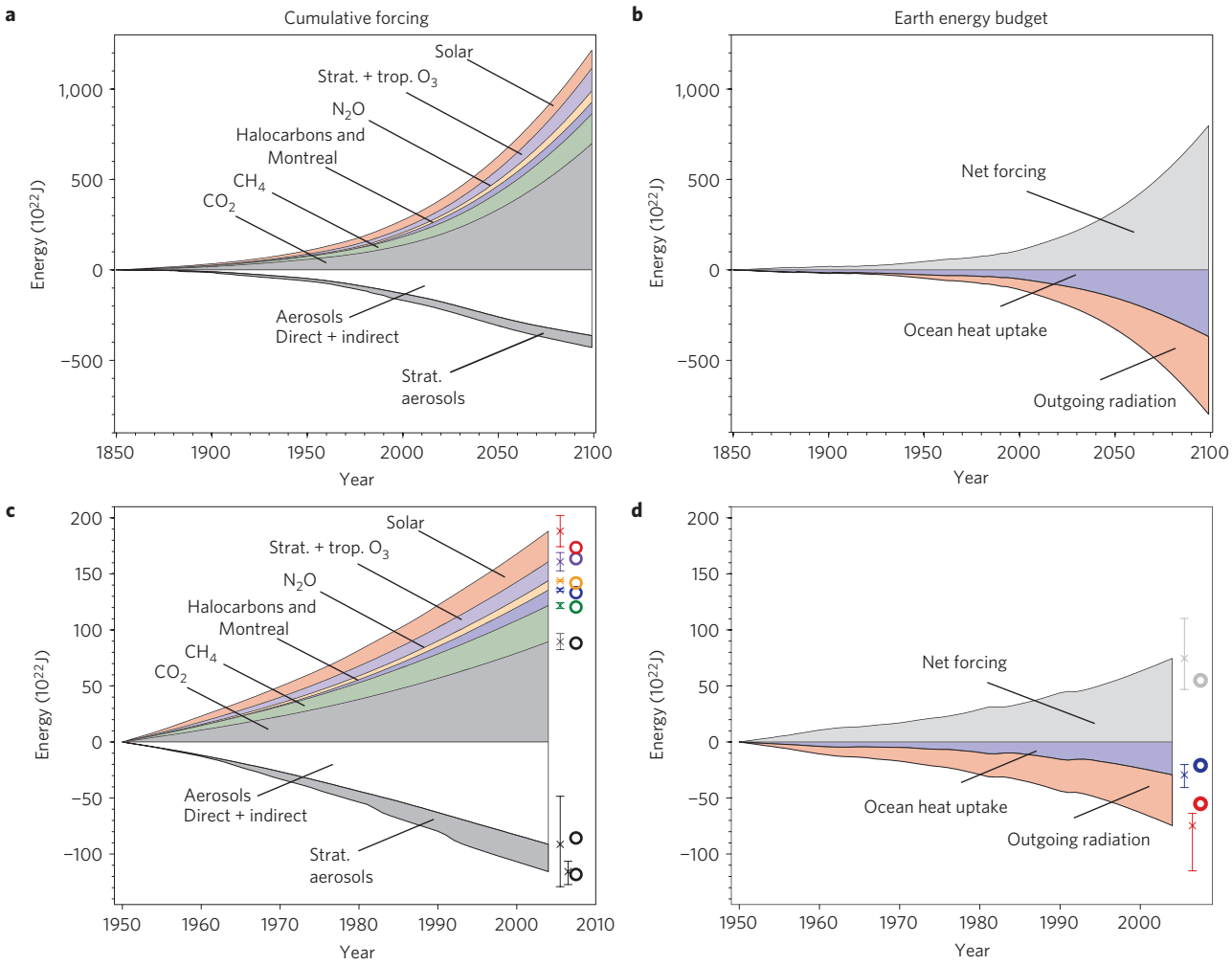

Figure 2 | Probabilistic estimates of the historical and future cumulative radiative forcing and the Earth's energy budget. a,**b**, Composition of the cumulative forcing energy (**a**) and the Earth's energy budget (**b**), given by eq. (1), during the years 1850–2100 for historical forcing and the SRES A2 scenario. **c**,**d**, Comparison of the simulated results with observations (circles[2]) for 1950–2004. The error bars denote the 5–95% uncertainty range of the probabilistic estimates.

in Fig. 3d. Under the SRES A2 scenario the temperature change by 2050–2059 of 1.29 (0.94–1.60) °C compared to the 2000s is almost entirely due to increasing greenhouse gas forcing. The cooling effects of aerosols and other negative forcing agents, as well as of other positive forcing agents, depend on the particular choice of the scenario, and the A2 case is simply one illustrative case. However, it demonstrates the overwhelming contribution of greenhouse gases, and CO_2 in particular, for non-intervention scenarios. The warming induced by CO_2 will also persist for at least a thousand years as a result of the slow ocean carbon uptake, far longer than the warming from most other forcing agents[22]. This emphasizes the need to focus on CO_2 in mitigating climate change. The projections under the SRES A2 scenario based on this method are very similar to estimates from a range of different climate models and statistical methods[17].

The basis for our energy balance model and a crucial step in determining the contributions of anthropogenic and natural (solar and volcanic) forcings to the observed changes is the magnitude of the internal unforced variability of global temperature and energy content. Figure 4 compares the observed trends in global average temperature and energy content over the past 50 years with the distribution of 50-year linear trends derived from unforced control runs in the World Climate Research Programme's (WCRP) phase 3 Climate Model Intercomparison Project (CMIP3; ref. 23). The bottom panels show the upper 95% quantiles of the distribution for all timescales and each model, along with the corresponding values for the observed surface temperature (from 2009 backwards) and ocean heat uptake to 700 m (from 2007 backwards). For global surface temperature it is extremely unlikely (<5% probability) that internal variability contributed more than $26 \pm 12\%$ and $18 \pm 9\%$ to the observed trends over the last 50 and 100 years, respectively. Even if models were found to underestimate internal variability by a factor of three, it is extremely unlikely that internal variability could produce a trend as large as observed. This is consistent with reconstructions over the last millennium indicating relatively small temperature variations that can mostly be explained by solar and volcanic forcing[24]. The ocean warming is similarly anomalous, but observations are more uncertain and the evaluation of model variability more difficult.

The Intergovernmental Panel on Climate Change (IPCC) states in its Fourth Assessment Report (AR4; ref. 8) that 'most of the observed increase in global average temperatures since the mid-twentieth century is very likely due to the observed increase in anthropogenic greenhouse gas concentrations', that 'it is likely that increases in greenhouse gas concentrations alone would have caused more warming than observed', and that 'it is extremely unlikely that global climate change of the past 50 years can be explained without

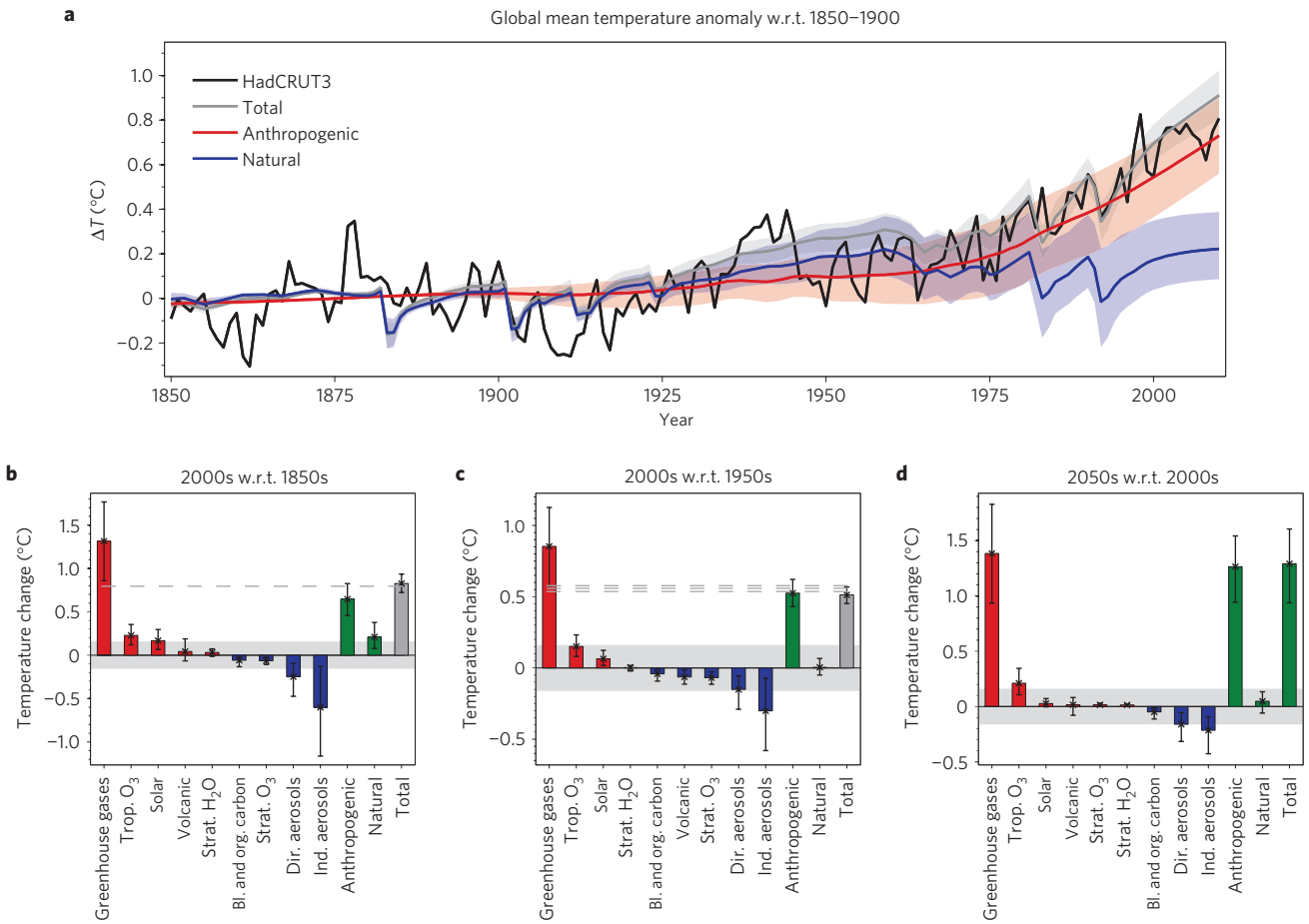

Figure 3 | Contributions of different forcing agents to the total observed temperature change. a, Time series of anthropogenic and natural forcings contributions to total simulated and observed global temperature change. The coloured shadings denote the 5-95% uncertainty range. **b**–**d**, Contributions of individual forcing agents to the total decadal temperature change for three time periods. Error bars denote the 5–95% uncertainty range. The grey shading shows the estimated 5–95% range for internal variability based on the CMIP3 climate models. Observations are shown as dashed lines.

external forcing, and very likely that it is not due to known natural causes alone'. Those results were predominantly driven by optimal fingerprinting studies.

Here we have shown that for global temperature the fundamental principle of conservation of energy, combined with knowledge about the evolution of radiative forcing, provides a complementary approach to attribution. Our results are strongly constrained by global observations and are robust when considering uncertainties in radiative forcing, the observed warming and in climate feedbacks. Each of the thousands of model simulations is a consistent realization of the ocean atmosphere energy balance. The resulting distribution of climate sensitivity (1.7–6.5 °C, 5–95%, mean 3.6 °C) is also consistent with independent evidence derived from palaeoclimate archives[11]. Using a more informative prior assumption does not significantly alter the conclusions (see Supplementary Information). Our results show that it is extremely likely that at least 74% (±12%, 1σ) of the observed warming since 1950 was caused by radiative forcings, and less than 26% (±12%) by unforced internal variability. Of the forced signal during that particular period, 102% (90–116%) is due to anthropogenic and 1% (−10 to 13%) due to natural forcing. The discrepancy between the total and the sum of the two contributions (14% on average) arises because the total ocean heat uptake is different from the sum of the responses to the individual forcings. Even for a reconstruction with high variability in total irradiance, solar forcing contributed only about 0.07 °C (0.03–0.13 °C) to the warming since 1950 (see Fig. 3c). The combination of those results with attribution studies based on optimal fingerprinting, with independent constraints on the magnitude of climate feedbacks, with process understanding, as well as palaeoclimate evidence leads to an even higher confidence about human influence dominating the observed temperature increase since pre-industrial times.

Methods

We use the Bern2.5D Earth system model of intermediate complexity, which is based on a zonally averaged dynamic ocean model. The ocean basins of the Atlantic, Pacific, Indian and Southern oceans are resolved and are coupled to a zonally and vertically averaged energy and moisture-balance model of the atmosphere[12,25]. The prescribed historical natural and anthropogenic radiative forcings used to drive the climate model are based on refs 16 and 15 and are identical to ref. 26.

The implementation and prior distributions of scaling factors in the Bern2.5D climate model, which account for the uncertainty in different forcing agents, are described in detail in ref. 17. In total, twelve parameters are sampled in the model: three physical parameters, including climate sensitivity, vertical ocean diffusivity and the transfer coefficient for sensible heat, as well as nine forcing scaling parameters accounting for forcing uncertainty (for example, of greenhouse gases, direct and indirect aerosol effects, volcanic eruptions and solar variations). It is assumed that the feedbacks are constant over time and the forcing uncertainty can largely be captured by a time-independent scaling factor. The shape of the forcing time series is not changed. Large prior uncertainties in the scaling factor are chosen to account for efficacies potentially being different for different forcings. Further details on the model, method, forcing and observations are given in refs 13,17,26.

The replacement of the full Bern2.5D with a neural network (NN) substitute is described in ref. 17. A 3-layer feed-forward neural network built of 10 nodes is trained with 5,000 time series of the Bern2.5D model output. A network is trained separately for global-mean temperature, ocean heat content to 700 m and

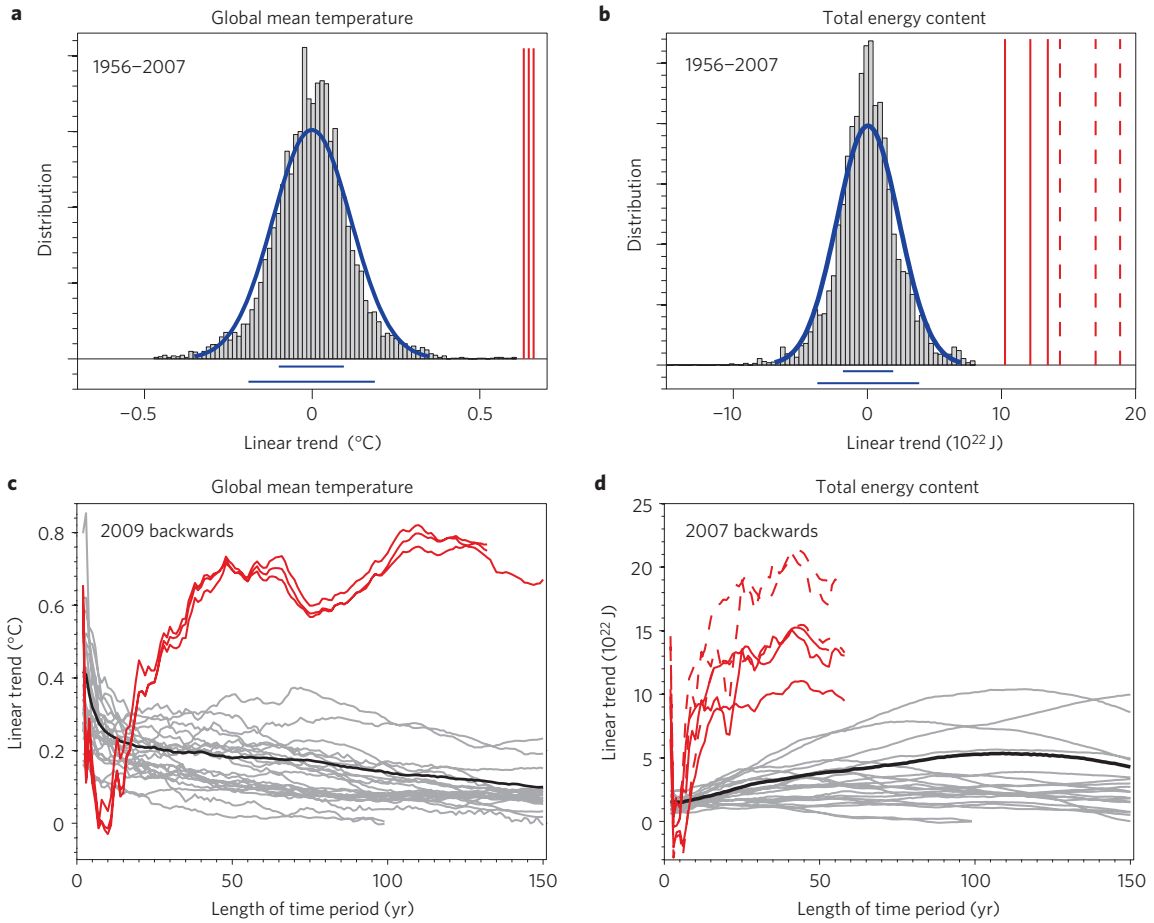

Figure 4 | Comparison of observed changes in global mean temperature and energy content with model estimates of internal variability. a,**b**, Distribution of linear trends for surface temperature and total energy content from unforced control simulations (grey bars) and observations (red lines) during 1956–2007. **c**,**d**, Upper 95% percentile as in **a**,**b** estimated for each CMIP3 model (grey lines). Observations are shown in red. **b**,**d**, Observations of the ocean heat uptake to 700 m are compared with the net radiation imbalance of the CMIP3 models. The total energy content of the Earth is difficult to measure but is about 40% higher than the 700 m heat uptake, which is indicated in **b**,**d** as dashed lines.

the temperature increase under a 1% to double CO_2 compared to pre-industrial atmospheric concentrations. In terms of global temperature, the annual error of the neural network is of the order of 0.1 °C, which is of the same magnitude as the error of current observational datasets and internal variability.

In ref. 17, the Bern2.5D model is constrained to a set of observational datasets, including the HadCRUT3 dataset of the Met Office Hadley Centre, the GISS Surface Temperature Analysis (GISTEMP) of the National Aeronautics and Space Administration and data of the National Oceanic and Atmospheric Administration (NOAA) National Climatic Data Center (NCDC). Ocean heat uptake observations include datasets of refs 3,27–29. Each combination of these datasets constitutes a plausible observational constraint. Best-guess estimates for the climate model parameters are derived from the aggregation of the posterior distributions from the individual dataset combinations.

The twelve model parameters in the Bern2.5D model are constrained with the Markov Chain Monte Carlo Algorithm (MCMC) described in ref. 17. The full climate model is replaced with its NN substitute to decrease the computational time of the algorithm. Within the parameter estimation process, uncertainties from observations, unforced internal variability and the neural network substitute are taken into account. At the core of the MCMC algorithm is the comparison of the model output for a given parameter combination with the observational datasets, thereby weighing the model parameters and their output according to their ability to reproduce past trends of global-mean surface air temperature and ocean heat uptake to 700 m (ref 17).

The contributions of the individual forcing species to the total temperature change is computed with nine single-forcing NNs with a network for each of the nine forcing agents (for example, greenhouse gases and aerosols). Climate sensitivity, vertical ocean diffusivity and the transfer coefficient for sensible heat are sampled in each single-forcing network. All NNs perform better than 0.01 $°C^2$, expressed by the mean squared error, which is about the same magnitude as the observed interannual variability of global-mean temperature. As the Bern2.5D climate model does not feature interannual variability, the temperature evolution is basically determined by climate sensitivity and vertical ocean diffusivity, which are sampled in each single-forcing NN. The single-forcing temperature contributions can subsequently be computed from the joint posterior distribution of the parameters. Here, we take the aggregated posterior distribution of the individual dataset combinations.

Received 21 June 2011; accepted 21 October 2011; published online 4 December 2011

References

1. Trenberth, K. E., Fasullo, J. T. & Kiehl, J. Earth's global energy budget. *Bull. Am. Meteorol. Soc.* **90,** 311–323 (2009).
2. Murphy, D. M. *et al.* An observationally based energy balance for the Earth since 1950. *J. Geophys. Res.* **114,** D17107 (2009).
3. Domingues, C. M. *et al.* Improved estimates of upper-ocean warming and multi-decadal sea-level rise. *Nature* **453,** 1090–1093 (2008).
4. Hegerl, G. C. *et al.* in *IPCC Climate Change 2007: The Physical Science Basis* (eds Solomon, S. *et al.*) (Cambridge Univ. Press, 2007).
5. Tett, S. F. B., Stott, P. A., Allen, M. R., Ingram, W. J. & Mitchell, J. F. B. Causes of twentieth-century temperature change near the Earth's surface. *Nature* **399,** 569–572 (1999).
6. Stott, P. A. *et al.* Attribution of twentieth century temperature change to natural and anthropogenic causes. *Clim. Dyn.* **17,** 1–21 (2001).
7. Barnett, T. *et al.* Detecting and attributing external influences on the climate system: A review of recent advances. *J. Clim.* **18,** 1291–1314 (2005).
8. Solomon, S. *et al.* in *IPCC Climate Change 2007: The Physical Science Basis* (eds Solomon, S. *et al.*) (Cambridge Univ. Press, 2007).
9. Levitus, S., Antonov, J. & Boyer, T. Warming of the world ocean, 1955–2003. *Geophys. Res. Lett.* **32,** L02604 (2005).
10. Lyman, J. M. *et al.* Robust warming of the global upper ocean. *Nature* **465,** 334–337 (2010).

11. Knutti, R. & Hegerl, G. C. The equilibrium sensitivity of the Earth's temperature to radiation changes. *Nature Geosci.* **1,** 735–743 (2008).
12. Stocker, T. F., Wright, D. G. & Mysak, L. A. A zonally averaged, coupled ocean atmosphere model for paleoclimate studies. *J. Clim.* **5,** 773–797 (1992).
13. Knutti, R., Stocker, T. F., Joos, F. & Plattner, G. K. Constraints on radiative forcing and future climate change from observations and climate model ensembles. *Nature* **416,** 719–723 (2002).
14. Nakicenovic, N. & Swart, R. Special Report on Emissions Scenarios. A Special Report of Working Group III of the Intergovernmental Panel on Climate Change (2000).
15. Joos, F. *et al.* Global warming feedbacks on terrestrial carbon uptake under the Intergovernmental Panel on Climate Change (IPCC) emission scenarios. *Glob. Biogeochem. Cycles* **15,** 891–907 (2001).
16. Crowley, T. J. Causes of climate change over the past 1000 years. *Science* **289,** 270–277 (2000).
17. Huber, M. B. *The Earth's Energy Balance and its Changes: Implications for Past and Future Temperature Change* http://dx.doi.org/10.3929/ethz-a-006689560 (ETH, 2011).
18. Baringer, M. O., Arndt, D. S. & Johnson, M. R. State of the Climate in 2009. *Bull. Am. Meteorol. Soc.* **91,** S1–S224 (2010).
19. Hansen, J. *et al.* Efficacy of climate forcings. *J. Geophys. Res.* **110,** D18104 (2005).
20. Stone, D. A., Allen, M. R., Selten, F., Kliphuis, M. & Stott, P. A. The detection and attribution of climate change using an ensemble of opportunity. *J. Clim.* **20,** 504–516 (2007).
21. Meinshausen, M. *et al.* Greenhouse-gas emission targets for limiting global warming to 2 °C. *Nature* **458,** 1158–1162 (2009).
22. Solomon, S., Plattner, G. K., Knutti, R. & Friedlingstein, P. Irreversible climate change due to carbon dioxide emissions. *Proc. Natl Acad. Sci. USA* **106,** 1704–1709 (2009).
23. Meehl, G. A., Covey, C., McAvaney, B., Latif, M. & Stouffer, R. J. Overview of the coupled model intercomparison project. *Bull. Am. Meteorol. Soc.* **86,** 89–93 (2005).
24. Hegerl, G. C., Crowley, T. J., Hyde, W. T. & Frame, D. J. Climate sensitivity constrained by temperature reconstructions over the past seven centuries. *Nature* **440,** 1029–1032 (2006).
25. Schmittner, A. & Stocker, T. F. The stability of the thermohaline circulation in global warming experiments. *J. Clim.* **12,** 1117–1133 (1999).
26. Knutti, R., Stocker, T. F., Joos, F. & Plattner, G. K. Probabilistic climate change projections using neural networks. *Clim. Dyn.* **21,** 257–272 (2003).
27. Levitus, S. *et al.* Global ocean heat content 1955–2008 in light of recently revealed instrumentation problems. *Geophys. Res. Lett.* **36,** L07608 (2009).
28. Ishii, M. & Kimoto, M. Reevaluation of historical ocean heat content variations with time-varying XBT and MBT depth bias corrections. *J. Oceanogr.* **65,** 287–299 (2009).
29. Palmer, M. D., Haines, K., Tett, S. F. B. & Ansell, T. J. Isolating the signal of ocean global warming. *Geophys. Res. Lett.* **34,** L23610 (2007).

Acknowledgements

We thank Urs Beyerle for the technical support of the climate model. Support for the International Detection and Attribution Working Group (IDAG) by the US Department of Energy's Office of Science, Office of Biological and Environmental Research grant DE-SC0004956 and the National Oceanic and Atmospheric Administration's Climate Program Office is acknowledged.

Author contributions

M.H. performed the climate model computations and statistical analysis. Both authors designed the study and wrote the paper.

Additional information

The authors declare no competing financial interests. Supplementary information accompanies this paper on www.nature.com/naturegeoscience. Reprints and permissions information is available online at http://www.nature.com/reprints. Correspondence and requests for materials should be addressed to R.K.